

Pd-supported on sulfated monoclinic zirconia for the reduction of NO₂ with methane under lean conditions

Erik M. Holmgreen, Matthew M. Yung, and Umit S. Ozkan*

Department of Chemical and Biomolecular Engineering, The Ohio State University, Columbus, OH, 43210, USA

Received 7 June 2006; accepted 5 August 2006

NO₂ reduction with methane under lean conditions is studied as a part of a two-stage scheme where NO is first oxidized to NO₂ over an oxidation catalyst and NO₂ is subsequently reduced to N₂ over a reduction catalyst. Pd supported on a sulfated monoclinic zirconia support was observed to have good activity for the reduction of NO₂ with CH₄ under lean conditions, giving N₂ yields over 60% over a broad temperature range below 450 °C. Sulfate groups are shown to be thermally stable below the calcination temperature.

KEY WORDS: NO₂ reduction; methane; sulfated zirconia; monoclinic.

1. Introduction

Nitrogen oxides (NO_x) represent a significant environmental pollutant, contributing to the formation of acid rain, smog, and ground level ozone. As such they have received much regulatory and research attention. Hydrocarbons in particular have been studied as potential NO_x reducing agents, with methane being a focus due to its relative low cost and widespread availability [1–5]. A significant challenge to the use of methane as a reducing agent is the presence of excess oxygen (lean conditions) in many combustion exhaust streams, as under lean conditions methane tends to preferentially combust with oxygen [6,7]. We have previously demonstrated a series of Pd-based catalysts were active for the reduction of NO with CH₄, although activity was highly dependant on the oxidation state of Pd [8–10]. Addition of Gd to this system was shown to improve O₂ tolerance and maintain activity under lean conditions [11]. On H-ZSM-5 supported Pd, Nishizaka and Misono [12,13] discovered a link between high N₂ selectivity in excess O₂ and acidity of the support material. Loughran and Resasco [14] also observed activity over other acidic supports, including sulfated zirconia. Further work by Resasco *et al.* showed that acidic supports served to stabilize Pd as active 2+ ions, while over non-acidic supports PdO clusters were formed and were responsible for CH₄ combustion [15]. Sulfated zirconia was further shown to maintain activity as well or better than zeolitic supports in the presence of H₂O and SO₂ [16–18].

The most common preparation method of sulfated zirconia is exposure of ZrOH to either sulfuric acid [19] or ammonium sulfate [20]. Upon calcination, the tetragonal zirconia crystal phase is preferentially formed, and it is believed to be stabilized by the presence of sulfate groups [21]. However, the tetragonal phase is thermodynamically stable only at high temperatures. Under common reaction conditions zirconia transitions to the monoclinic phase, which has been shown to be less active in acid catalyzed reactions [22], although not completely inactive [23]. Loss of activity for the NO reduction reaction has been attributed to this transition [24].

Previously we have introduced a two-stage approach to the reduction of NO with hydrocarbons [25], in which NO would first be oxidized to NO₂ over an oxidizing catalyst and NO₂ reduced with hydrocarbons over a reduction catalyst. The rationale for the approach was that NO₂ is a stronger oxidizing agent, and therefore should be better able to compete with O₂ for use of CH₄. Improved performance for the reduction of NO₂ with hydrocarbons has been observed in the literature [26,27]. In this article we present results on the activity of Pd-based sulfated monoclinic zirconia catalysts for the reduction of NO₂ with CH₄. Although the tetragonal zirconia support has been shown to be more active, in this study, we have chosen to use the monoclinic phase, which is the more stable form. Since reduction of NO₂ is easier than that of NO, the monoclinic phase may still be effectively used in a two-stage system where the oxidation of NO to NO₂ will take place over an oxidation catalyst. Studies performed incorporating these catalysts with an NO oxidation catalyst into a two-catalyst system for the reduction of NO will be presented in the next article in the series.

*To whom correspondence should be addressed.
E-mail: ozkan.1@osu.edu

2. Experimental

2.1. Catalyst preparation

Palladium-based sulfated zirconia catalysts were prepared over a commercial monoclinic zirconia support, supplied by Saint-Gobain. The zirconia was received in pelletized form, and the first preparation step was to grind and screen the support. The 100–140 mesh cut (0.149–0.105 mm) was saved, then calcined in air for 3 h at 500 °C. The calcined powder was screened a second time and the 100–140 mesh cut was used for catalyst preparation.

Sulfated zirconia supports were prepared to a nominal 5 wt% loading of sulfate through a standard incipient wetness technique. Incipient wetness was performed using an aqueous solution of ammonium sulfate (99 + %, Sigma-Aldrich). A solution volume equal to the pore volume of the catalyst was added drop wise, and the powder thoroughly mixed. After addition of ammonium sulfate the samples were dried at 110 °C overnight. After drying the sulfated zirconia samples were calcined in air for 3 h at 500 °C. Palladium addition was performed through the same incipient wetness technique using a solution of palladium chloride (59% Pd, MCB Reagents) or palladium nitrate (Aldrich). After addition of the palladium the samples were again dried at 110 °C overnight, and then were calcined in air at 500 °C for 3 h. Catalysts were prepared using 5% SZ at palladium loadings of 0.1%, 0.3%, and 0.5% by weight.

2.2. BET surface area measurements

Catalyst surface areas were measured through N₂ physisorption on a Micromeritics ASAP 2010. Samples were degassed overnight at 130 °C and 3 μm Hg before analysis.

2.3. Catalytic activity testing

Catalyst activity measurements were performed in a packed bed reactor made of ¼ in. o.d. stainless-steel tubing. Catalyst samples (0.2 g) were packed into the reactor between two plugs of quartz wool. Reaction temperature was measured using a K-type thermocouple in contact with one of the quartz plugs, and controlled using an Omega 76000 temperature controller. Activity was measured in the temperature range of 200–450 °C in 25 °C increments. At each temperature final product analysis was performed at steady-state, which was reached generally after 1–2 h. Independent Brooks 5850E mass flow controllers, connected to a Brooks 0154 electronics control box, were used to control feed gas concentrations and total flow rate. All reactant gases were purchased from Praxair. Reaction conditions for the steady-state reaction studies were 1000 ppm NO or NO₂, 3000 ppm CH₄, and 10% O₂ in balance He. The total flow rate corresponded to a GHSV of 20,000 h⁻¹.

Before each reaction experiment the catalyst samples were pretreated in 10% O₂/He at 400 °C, for 30 min. Feed stream and product analysis was performed using a combination of techniques. Quantification of O₂, N₂, N₂O, CH₄, CO, and CO₂ was performed using a Varian CP4900 MicroGC. NO and NO₂ were monitored with a Thermo Environmental Model 42H chemiluminescence NO_x detector. Additionally, in several experiments a Siemens infrared NH₃ analyzer was used. However NH₃ was never detected in the product stream. Reactant conversions were calculated as (1-outlet/inlet)*100%. N₂ yields were calculated as (2 × N₂ produced/NO_x fed)*100%.

2.4. Controlled atmosphere X-ray diffraction

The stability of the zirconia crystalline phase was confirmed using a Bruker D8 Advanced X-ray diffractometer equipped with a Cu Kα source and a position sensitive detector. *In situ* diffraction patterns of the sulfated zirconia sample were taken during calcinations under controlled atmosphere and controlled temperature conditions using a HTK 1200 sample holder. The sample was maintained under a flow of air at approximately 15 mL/min. The sample temperature was raised at 3 °C/min in 50 °C increments with a 10-min pause to allow for temperature equilibration. After the 10-min hold a diffraction pattern was taken. Diffraction data were taken between 50–750 °C.

2.5. X-ray photoelectron spectroscopy

XPS experiments were performed on an AXIS Ultra instrument, using a monochromatic Al anode. Sample powders were supported on double-sided carbon tape. After the data collection charge shift corrections were performed using the standard C 1s binding energy of 284.5 eV.

2.6. Temperature programmed desorption

TPD studies were performed using a Finnigan Trace DSQ mass spectrometer. For each experiment 0.1 g of catalyst sample was placed in a quartz U-tube reactor between plugs of quartz wool. Samples were pretreated under 10% O₂/He, held at 400 °C for 30 min. The catalyst was then cooled to room temperature in He. The samples were then exposed to either He or 10% O₂/He, and the desorption of sulfur species was monitored by mass spectrometer. Experimental conditions were 30 cm³/min flow of gas, and a temperature ramp rate of 10 °C/min.

2.7. Diffuse reflectance infrared Fourier transform spectroscopy

DRIFTS experiments were performed with a Bruker IFS66 instrument using equipped with an MCT detector. For all samples the final spectrum was averaged

over 1000 scans. Pd/SZ was mixed at 15 wt% with ground KBr. A sample of this mixture was placed in a heated sample cup inside a Spectratech diffuse reflectance cell. Samples were treated in 10% O₂ at 100 °C for 30 min before spectra were taken. Samples were then cooled to room temperature under He. For the NO and NO₂ adsorption experiments the species were adsorbed for 30 min at a concentration of 1000 ppm, and the sample was then flushed with He for 30 min.

3. Results

3.1. Catalyst preparation

Table 1 shows BET surface area results for the commercial monoclinic ZrO₂ support, as well as the three Pd/SZ catalysts with different Pd loadings. The loading levels were kept very low, with the maximum being 0.5 wt%. The surface area for the commercial support was taken after the sieving and calcination procedure used to prepare it. The low metal and sulfate loadings resulted in very little surface area difference among the catalysts.

The addition of surface acidity through the presence of sulfate groups is known to be key in determining activity for NO_x reduction with methane. Several experiments were performed to examine the effect of preparation steps and preparation parameters of the sulfated zirconia catalysts, specifically the behavior of surface sulfur species. These species are known to be thermally unstable; so the effect of calcination temperature was examined through temperature-programmed techniques. Dried, but uncalcined samples of sulfated zirconia were treated in flows of He and 10% O₂/He while the effluent was analyzed by on-line mass spectrometry. Figure 1 shows the data for *m/e* = 64, corresponding to SO₂ taken under O₂/He and He-only atmospheres. The desorption profiles for under each atmosphere revealed a strong maximum around 525 °C. This was the only desorption feature observed under O₂/He atmosphere below 650 °C. During the treatment with He, however, desorption of SO₂ was initially observed just above 250 °C. Two additional small features were also observed, a peak at 350 °C and a shoulder at 440 °C. There was also a shoulder seen around 600 °C. The final desorption feature which begins around 650 °C is due to thermal decomposition

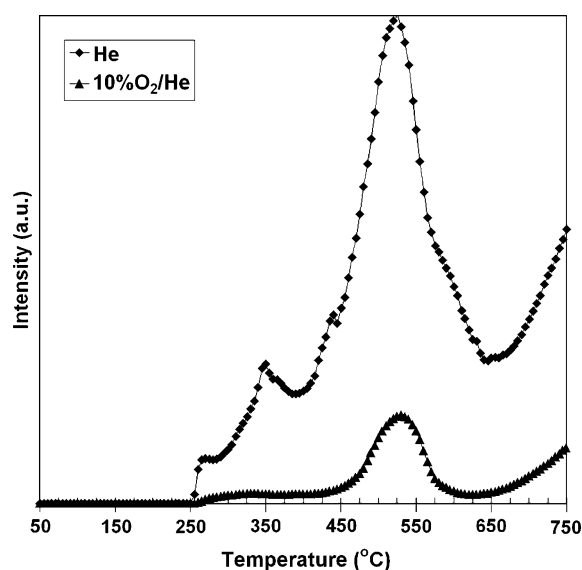


Figure 1. TPD of SO₂ (*m/e* = 64) during the heat treatment of impregnated and dried sulfated zirconia. Samples were treated under He (♦) and 10% O₂/He (▲).

and is seen under both atmospheres. In both experiments the ion for SO (*m/e* = 48) was observed to match that of SO₂, indicating that it was present due to fragmentation. The most significant difference between the two pretreatment atmospheres however is the large intensity difference. When treated under He the loss of sulfur species is several times greater across the entire temperature range. The low temperature desorption of SO₂ and the higher intensity under He suggests that O₂ can be stabilizing the surface sulfate groups. We therefore conclude that the majority of the added sulfate is thermally stable under O₂ pretreatment up to 650 °C.

Confirmation of this conclusion was provided by XPS spectra taken of the Pd/SZ catalyst at each of the five separate synthesis steps. Spectra of the Zr3d, S2p, and O1s regions were taken of the untreated commercial ZrO₂ sample, the sulfated but uncalcined sample, calcined sulfated zirconia, loaded but uncalcined 0.5% Pd/SZ, and the final 0.5% Pd/SZ catalyst. These results are shown in Figures 2–4, respectively. In Figure 2 the Zr3d_{5/2} peak is located at a binding energy of 182.1 eV, typical for ZrO₂. After treatment with ammonium sulfate and drying, a shift to higher binding energy was observed. The 5/2 peak was shifted to 182.9 eV. This increase in binding energy is due to a decrease in electron density as a result of increased surface acidity [28]. The shift was stable through the subsequent catalyst preparation steps, indicating stable surface conditions. Examination of the S2p region in Figure 3 shows direct evidence of stable sulfate species. As expected, no peak was observed in this region on the commercial ZrO₂ sample. Upon the addition of ammonium sulfate, a relatively broad peak centered on 169.3 eV is visible. Such a peak falls in the standard

Table 1

BET surface areas of the unloaded support and the prepared Pd/SZ catalysts

| Catalyst | BET SA (m ² /g) |
|-----------------------------|----------------------------|
| Commercial ZrO ₂ | 48.4 |
| 0.1% Pd/SZ | 48.0 |
| 0.3% Pd/SZ | 47.9 |
| 0.5% Pd/SZ | 46.3 |

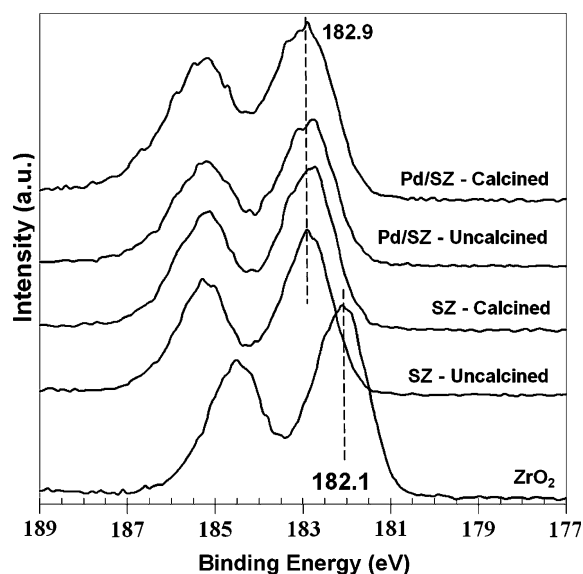


Figure 2. Zr3d region of the X-ray photoelectron spectra of catalyst samples taken at each step in the synthesis procedure. From bottom to top: commercial monoclinic ZrO_2 , dried but uncalcined SZ, SZ support, impregnated but uncalcined 0.5% Pd/SZ, the final 0.5% Pd/SZ.

binding energy range of sulfur in metal sulfates. Through calcination of the sample and the addition of Pd, the intensity and location of this peak do not change. Splitting between the $2p_{3/2}$ and $2p_{1/2}$ was not observed due to relatively low counts in this region, and the close spacing of these peaks for sulfur. The O1s region presented in Figure 4 shows an increase in binding energy from 530.0 to 530.7 eV after sulfation. Such a shift is consistent with the observations made in the Zr3d region. Additionally, the growth of a shoulder at 531.9 corresponds to oxygen present in sulfate

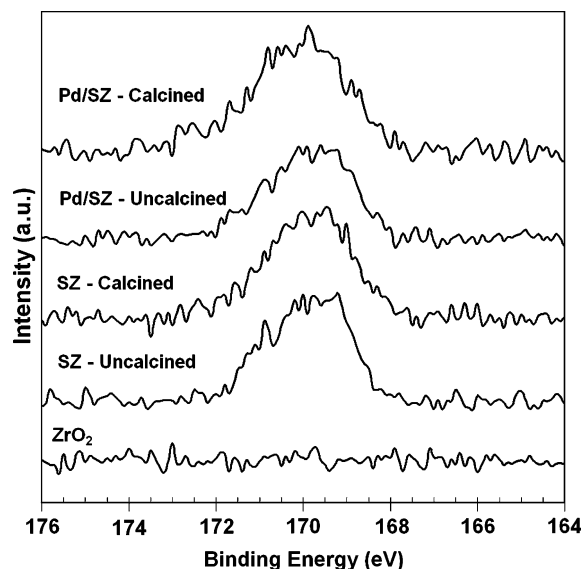


Figure 3. S2p region of the X-ray photoelectron spectra of catalyst samples taken at each step in the synthesis procedure. From bottom to top: commercial monoclinic ZrO_2 , dried but uncalcined SZ, SZ support, impregnated but uncalcined 0.5% Pd/SZ, the final 0.5% Pd/SZ.

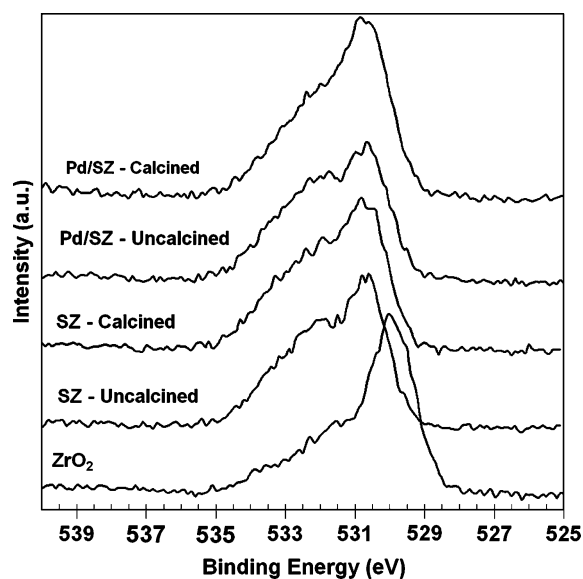


Figure 4. O1s region of the X-ray photoelectron spectra of catalyst samples taken at each step in the synthesis procedure. From bottom to top: commercial monoclinic ZrO_2 , dried but uncalcined SZ, SZ support, impregnated but uncalcined 0.5% Pd/SZ, the final 0.5% Pd/SZ.

species [29]. The observed peak shift and intensities are again constant with additional preparation steps.

In situ XRD during the calcination of sulfated zirconia was performed, and showed no evidence of a bulk crystalline change in the support. Beginning with an uncalcined sulfated zirconia sample, the calcination was performed under flowing air with diffraction patterns taken every 50 °C. Figure 5 contains a portion of this data, patterns taken every 100 °C. The range 20–70° 2θ is presented, and clearly show the presence of only monoclinic zirconia with peaks at 24, 28, and 31°.

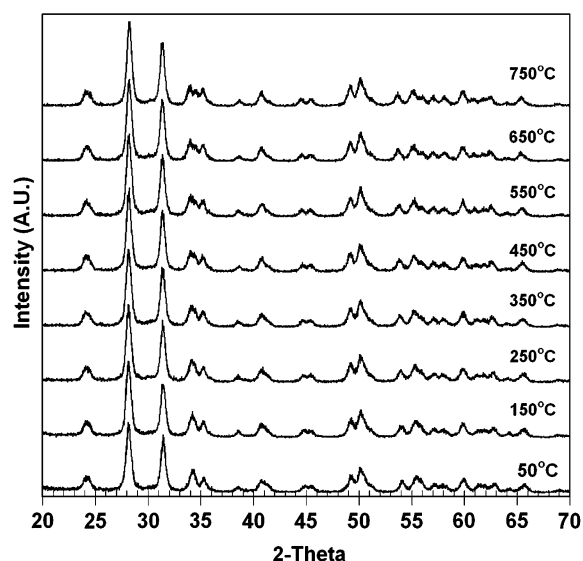


Figure 5. *In situ* XRD patterns taken during the calcination in air of sulfated zirconia.

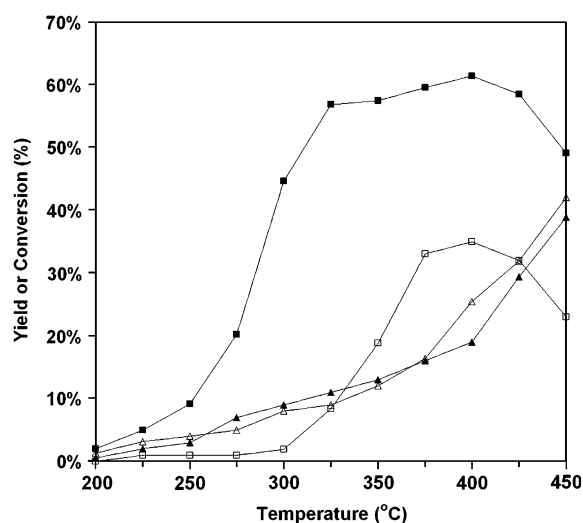


Figure 6. Steady-state reaction results from the reduction of NO (empty) and NO₂ (filled) with CH₄ over 0.1% Pd/SZ. N₂ yield (■, □) and CH₄ conversion (▲, Δ). Reaction conditions: 1000 ppm NO_x, 3000 ppm CH₄, 10% O₂ in He, GHSV = 20,000 h⁻¹.

3.2. Steady-state reaction experiments

The NO_x reduction activity of the Pd/SZ catalysts were tested in a feed containing 1000 ppm NO_x,

3000 ppm CH₄, and 10% O₂ in balance He. Figures 6 and 7 show results from these tests. Figure 6 shows a comparison of the activities for NO versus NO₂ reduction with CH₄ over 0.1% Pd/SZ catalyst. The N₂ yield and CH₄ conversion are plotted on the same graph for two different feed molecules. As shown in Figure 6, the catalyst has little activity for NO reduction until 325 °C. The maximum N₂ yield of 35% was observed at 400 °C, after which N₂ production decreased. NO conversion was very close to N₂ yield, although a small amount of N₂O was observed. For NO₂ conversion, on the other hand, there was reduction to N₂ at temperatures even as low as 200 °C, with a broad maximum over 325–425 °C range. The maximum N₂ yields achieved were much higher than those observed for NO reduction, reaching 57–61%. CH₄ conversions in the two experiments showed very similar trends, increasing with temperature, with a sharper light off observed above 375 °C and reaching conversion levels over 40% by 450 °C. The corresponding increase in CH₄ conversion with a decrease in N₂ yield is common in reactions performed with hydrocarbon reducing agents. Especially under lean conditions CH₄ combustion with O₂ becomes favored at higher temperatures.

NO₂ conversion was also monitored and revealed a significant side reaction. We observed the partial

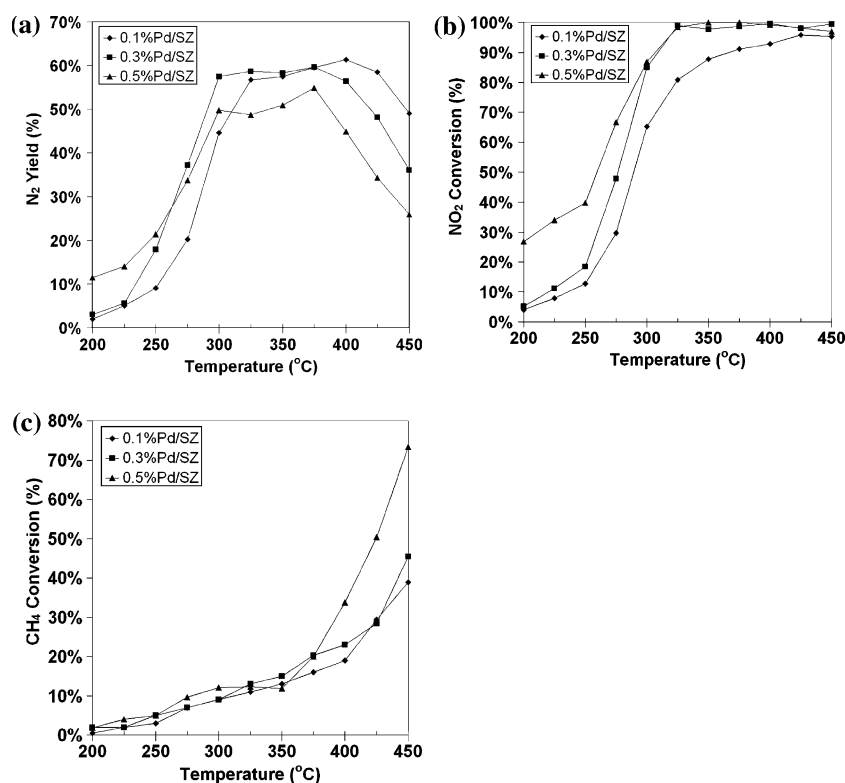


Figure 7. (a) Steady-state N₂ yields in the reduction of NO₂ with CH₄ over Pd/SZ catalysts. 0.5% Pd/SZ (▲), 0.3% Pd/SZ (■), and 0.1% Pd/SZ (◆). Reaction conditions: 1000 ppm NO, 3000 ppm CH₄, 10% O₂ in He, GHSV = 20,000 h⁻¹. (b) Steady-state NO₂ conversions in the reduction of NO₂ with CH₄ over Pd/SZ catalysts. 0.5% Pd/SZ (▲), 0.3% Pd/SZ (■), and 0.1% Pd/SZ (◆). Reaction conditions: 1000 ppm NO, 3000 ppm CH₄, 10% O₂ in He, GHSV = 20,000 h⁻¹. (c) Steady-state CH₄ conversions in the reduction of NO₂ with CH₄ over Pd/SZ catalysts. 0.5% Pd/SZ (▲), 0.3% Pd/SZ (■), and 0.1% Pd/SZ (◆). Reaction conditions: 1000 ppm NO, 3000 ppm CH₄, 10% O₂ in He, GHSV = 20,000 h⁻¹.

reduction of NO₂ to NO. Reaction tests (not shown) in which the CH₄ flow was stopped during the reaction confirmed that this was due to a reduction reaction, not due to NO₂ decomposition or NO–NO₂ equilibrium driven reactions. Almost complete NO₂ conversion occurred in the temperature range of the maximum in N₂ yield. In light of the improved activity for the reduction of NO₂ it seems that N₂ production may be capped by the complete removal of NO₂ by this side reaction. A large amount of NO is produced, which the catalyst is much less effective at reducing. Reaction with NO₂ also showed small quantities of N₂O formation. There was no NH₃ formation in either reaction.

The large difference observed in the N₂ yields in NO versus NO₂ reactions clearly confirms that NO₂ is much easier to reduce than NO. This result is important in validating the two-stage concept, which has been the basis for this study.

The effect of Pd loading on catalyst activity for the reduction of NO₂ with CH₄ was also investigated. Figure 7(a–c) show the steady-state reaction results obtained over catalysts with three different Pd loading levels. With both N₂ yield and NO₂ conversion, shown in Figure 7(a) and b, respectively, an increase in the catalyst Pd loading resulted in increased activity at low reaction temperatures. Over all three catalysts a broad maximum was observed in N₂ yield. For each of the three catalysts the maximum corresponded to high NO₂ conversions. This maximum on the 0.5% Pd/SZ occurred between temperatures of 300–375 °C, giving 47–53% N₂ yield. On 0.3% Pd/SZ yield reached a maximum in the same range, however it was higher, reaching 55–58%. In comparison to the higher loadings, the entire curve of N₂ yield with temperature was shifted to approximately 25 °C higher temperatures over the 0.1% Pd/SZ catalyst. The maximum N₂ yield was observed between 325 and 425 °C, reaching 55–60%. For all three catalysts, N₂ production dropped at high temperatures due to competition from the combustion reaction. Figure 7(c) shows the CH₄ conversions during NO₂ reduction. Below 400 °C conversion with all three Pd loadings was similar. At 400 °C a significant increase was observed on 0.5% Pd/SZ, which reached a conversion of 70% at 450 °C. With lower loading maximum CH₄ conversion dropped to 42% on 0.3% Pd/SZ and 39% on 0.1% Pd/SZ at the same temperature.

Comparisons of the results from these Pd loading levels indicate that with higher Pd content the two competitive reactions that bracket the maximum N₂ yield window are increased. The 0.5% Pd/SZ catalyst showed higher NO₂ conversion at low temperatures, much of which was converted to NO. Additionally at high temperatures the higher loading increased the rate of CH₄ combustion and decreased N₂ yield. Lowering the metal loading resulted in an increase in N₂ and a broadening of the activity temperature range.

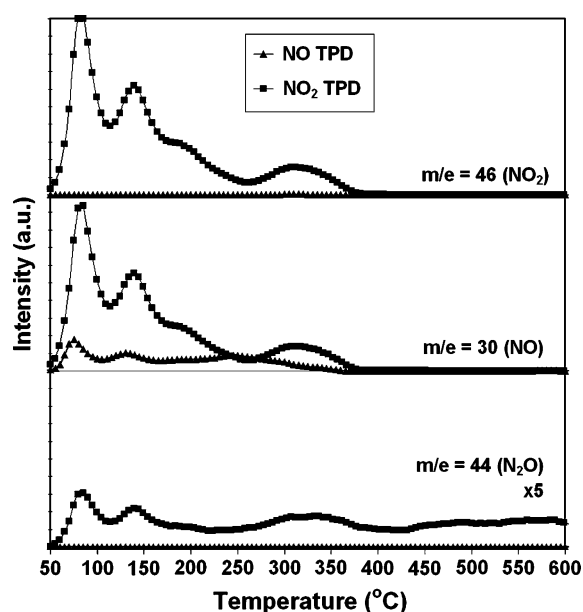


Figure 8. NO (▲) and NO₂ (■) TPD experiments from 0.5% Pd/SZ. Ions corresponding to $m/e = 46$ (NO₂), $m/e = 44$ (N₂O) and $m/e = 30$ (NO) are shown.

3.3. Temperature programmed desorption

The adsorption behavior and interactions of reactants with the catalyst surface were investigated through temperature programmed desorption techniques. Comparison of the desorption of NO and NO₂ from the 0.5% Pd/SZ catalyst is presented in Figure 8. The desorption profiles for $m/e = 46$ (NO₂), $m/e = 44$ (N₂O) and $m/e = 30$ (NO) are shown. Before the

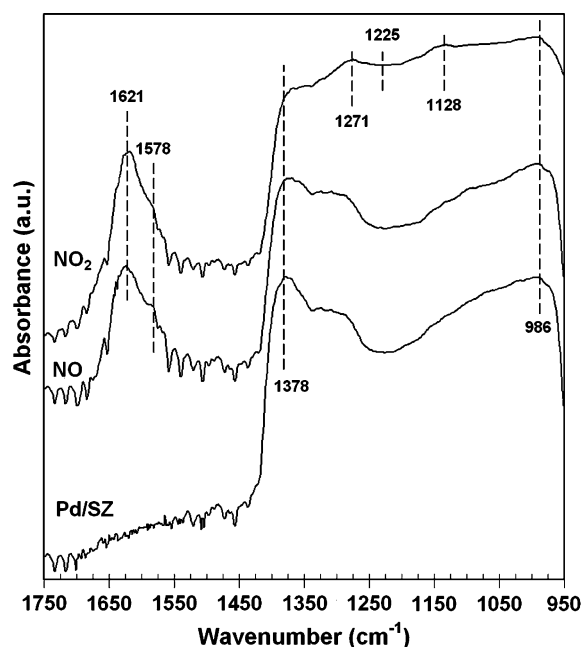


Figure 9. DRIFTS spectra of the Pd/SZ and KBr mixture. Spectra shown correspond to the sample, and following adsorption of NO or NO₂.

desorption experiments were performed, fragmentation of NO₂ by the mass spectrometer was determined and the NO₂:NO ratio was found to be 1.25:1. Following NO adsorption, neither NO₂ nor N₂O is observed, indicating that NO does not disproportionate on the catalyst surface. Three peaks are observed for the desorption of NO located at 75, 130, and 250 °C. TPD performed with NO₂ showed four desorption peaks for $m/e = 46$ at 85, 140, 190, and 320 °C, indicating significant levels of reversible adsorption for NO₂. Additionally NO₂ appears to undergo some rearrangement on the catalyst surface. Small amounts of both NO ($m/e = 30$) and N₂O ($m/e = 44$) were observed and the temperature of desorption for both of these species correspond closely with peaks for NO₂. The relative intensity of the NO signal is slightly higher than predicted by NO₂ fragmentation, indicating that, however small, some decomposition of NO does occur on the catalyst surface. The N₂O signal was small, and is multiplied by a factor of 5 in Figure 9 to make the peaks visible.

3.4. Diffuse reflectance Fourier transform spectroscopy

Figure 9 contains DRIFTS spectra for the 0.5% Pd/SZ catalyst after pretreatment and after adsorption of either NO or NO₂. In these experiments the catalyst was mixed to 15 wt% in KBr. The spectrum taken of the Pd/SZ catalyst shows a large absorption band at 1378 cm⁻¹. This band is due to S=O stretching of sulfate groups on the catalyst surface [30]. Additionally the feature in the range of 950–1200 cm⁻¹ can be assigned to S–O stretch [31]. These bands are typical for sulfated zirconia synthesized through other preparation routes, and confirm the presence of sulfate groups on the monoclinic support.

After exposure to NO several changes in the spectrum appear. The S=O stretch band at 1378 cm⁻¹ decreases in intensity. This decrease is due to a shift to lower wavenumber upon interaction with adsorbed NO. The formation of a strong band and shoulder at 1621 and 1578 cm⁻¹, respectively, are also observed. The band at 1621 cm⁻¹ is assigned to the formation of nitric acid [32] and corresponds to an intensity decrease in the hydroxyl region (not shown). The shoulder at 1578 cm⁻¹ is associated with the formation of bidentate nitrate species. Upon adsorption of NO₂, the band at 1378 cm⁻¹ decreases in intensity more sharply than in the NO experiment. Additionally, the bands at 1621 and 1578 cm⁻¹ are more intense. New bands 1271 and 1128 cm⁻¹ are observed and can be assigned to bidentate and bridged nitrates, respectively. In the region between these bands an increase in absorbance is also seen. A wavenumber of 1225 cm⁻¹ is assigned to the N–O stretch in N₂O [33].

Comparison of the NO and NO₂ adsorption experiments seem to indicate a stronger interaction of NO₂

with the sulfated zirconia, through a larger decrease in sulfate band intensity and a larger absorbance associated with surface nitrate species. These observations are consistent with the much larger NO₂ adsorption observed through temperature programmed desorption.

4. Conclusions

A simple incipient wetness impregnation method used with a commercial monoclinic support was demonstrated to produce a sulfated zirconia catalyst with good activity for the reduction of NO₂ with CH₄ under lean conditions. Characterization of this catalyst showed the formation of surface sulfate groups, and the corresponding surface acidity, that were thermally stable below the calcination temperature of 500 °C. N₂ yields of over 60% were achieved under a 10% O₂ feed (O₂:CH₄ > 30). Additionally the catalysts achieved maximum activity over a broad temperature range of 300–425 °C, depending on Pd content. This was observed to occur simultaneously within a temperature range of relatively low CH₄ and nearly complete NO₂ conversion. We believe that the activity is therefore limited at the low end by the competitive partial reduction of NO₂ to NO, and on the high end by the light off of CH₄ combustion with O₂. If the formation of NO is indeed limiting the yield of N₂, then incorporation into a system including a NO oxidation catalyst could be expected to increase performance. NO produced through the partial reduction could be quickly reoxidized. DRIFTS and TPD experiments examining the interaction of NO_x species with the Pd/SZ catalyst indicate a stronger surface interaction with NO₂, which may be significant in the improved reduction performance.

Acknowledgments

We would like to acknowledge the United States Department of Energy (DOE) and the National Energy Technology Laboratory (NETL) for funding this work through the cooperative agreement DE-FC26-02 NT41610.

References

- [1] Y. Li and J.N. Armor, *Appl. Catal. B: Environ.* 1 (1992) L31.
- [2] Y. Li, P.J. Battavio and J.N. Armor, *J. Catal.* 142 (1993) 561.
- [3] X. Zhang, A.B. Walter and M.A. Vannice, *Appl. Catal. B: Environ.* 4 (1994) 237.
- [4] R. Burch and A. Ramli, *Appl. Catal. B* 15 (1998) 49.
- [5] R. Burch and A. Ramli, *Appl. Catal. B* 15 (1998) 63.
- [6] M. Iwamoto and H. Hamada, *Catal. Today* 10 (1991) 57.
- [7] M. Iwamoto and H. Yahiro, *Catal. Today* 22 (1994) 5.
- [8] M.W. Kumthekar and U.S. Ozkan, *J. Catal.* 171 (1997) 45.
- [9] M.W. Kumthekar and U.S. Ozkan, *J. Catal.* 171 (1997) 54.
- [10] M.W. Kumthekar and U.S. Ozkan, *J. Catal.* 171 (1997) 67.

- [11] J. Mitome, E. Aceves and U.S. Ozkan, *Catal. Today* 53 (1999) 597.
- [12] Y. Nishizaka and M. Misono, *Chem Lett.* (1993) 1295.
- [13] Y. Nishizaka and M. Misono, *Chem Lett.* (1994) 2237.
- [14] C.J. Loughran and D.E. Resasco, *Appl. Catal. B* 7 (1995) 113.
- [15] A. Ali, W. Alvarez, C.J. Loughran and D.E. Resasco, *Appl. Catal. B* 14 (1997) 13.
- [16] Y.-H. Chin, A. Pisanu, L. Serventi, W.E. Alvarez and D.E. Resasco, *Catal. Today* 54 (1999) 419.
- [17] Y.-H. Chin, W.E. Alvarez and D.E. Resasco, *Catal. Today* 62 (2000) 159.
- [18] H. Ohtsuka, T. Tabata and T. Hirano, *Appl. Catal.* 28 (2000) L73.
- [19] K. Arata and M. Hino, *Appl. Catal.* 59 (1990) 197.
- [20] J.M. Parera, *Catal. Today* 15 (1992) 481.
- [21] W. Stichert and F. Schuth, *Chem. Mater.* 10 (1998) 2020.
- [22] D. Farcasiu, J.Q. Liu and S. Cameron, *Appl. Catal. A* 154 (1997) 173.
- [23] W. Stichert, F. Schuth, S. Kuba and H. Knozinger, *J. Catal.* 198 (2001) 277.
- [24] H. Ohtsuka, *Catal. Lett.* 87 (2003) 179.
- [25] E.M. Holmgreen, M.M. Yung and U.S. Ozkan, *Proceedings of ICEF04 ASME 2004 Fall Technical Conference* 893 (2004) 1.
- [26] F.C. Meunier and J.R.H. Ross, *Appl. Catal. B: Environ.* 24 (2000) –23.
- [27] H. Ohtsuka, *Appl. Catal. B: Environ.* 33 (2001) 325.
- [28] V. Quaschnig, J. Deutsch, P. Druska, H.-J. Niclas and E. Kemnitz, *J. Catal.* 177 (1998) 164.
- [29] M. Hino, M. Kurashige, H. Matsushashi and K. Arata, *Thermochim. Acta* 441 (2006) 35.
- [30] B. Tsytysarski, V. Avreyska, H. Kolev, Ts. Marinova, D. Klissurski and K. Hadjiivanov, *J. Mol. Catal. A: Chem.* 193 (2003) –139.
- [31] C. Morterra, G. Cerrato, F. Pinna and M. Signoretto, *J. Phys. Chem.* 98 (1994) 12373.
- [32] M. Kantcheva and E.Z. Ciftlikli, *J. Phys. Chem. B* 106 (2002) 3941.
- [33] K. Hadjiivanov, Va. Avreyska, D. Klissurski and T. Marinova, *Langmuir* 18 (2002) 1619.